Electronic Supplementary Material (ESI) for Journal of Materials Chemistry C.

Supplemental Information

Three-dimensional magnetite replicas of pollen particles with tailorable and predictable multimodal adhesion

Ismael J. Gomez‡[a], W. Brandon Goodwin‡[b], Dan Sabo[c], Z. John Zhang[c], Kenneth H. Sandhage*[b,c] and J. Carson Meredith*[a]

Additional Experimental Description

To allow for direct evaluation of the shape and feature retention of the same Fe-O-coated pollen grain before and after firing, nickel foil substrates were stamped with distinctive patterns, such as "X" patterns (as shown in Figure S1 below). A pipette was used to place a droplet, consisting of a mixture of coated pollen particles in anhydrous 2-propanol, onto the nickel foil and the alcohol was allowed to evaporate. Low and high magnification SE images were used to identify particular particles (as well as particular surface features on a given particle) and their locations relative to a given stamped pattern. After pyrolysis at 600°C and/or the Rhine's pack treatment at 550°C, similar SE images were again obtained to help locate particular individual grains and to evaluate the quality of replication (e.g., higher magnification SE images were used to identify whether particular surface features on a particular pollen grain replica were retained). Many of the pollen grains remained in the same location after pyrolysis (see the grains marked 1, 2, and 3 in Figure S1a and b), which allowed for unambiguous evaluation of the shape and feature retention upon pyrolysis of these grains.

The diameters of the SSG-coated pollen and oxide pollen replicas were determined by fitting a circle around the pollen grain echini and measuring the diameter of the circle, as shown in S2. The diameters of the same pollen grains were compared to each other before and after each thermal treatment.

Additional Modelling Description

In order to calculate the magnetic volume (V_m) of a particular Fe_3O_4 pollen replica particle from eqn (2), the $\partial H/\partial z$ term must be determined. Therefore, the magnetostatic potential (Φ) and magnetic field (H) around the Ni-Nd substrate were modelled using the methodology adapted from the work of Leventis, et al.[11] Because H is related to Φ by eqn (4), Φ must first be evaluated from the expression in eqn (3). The expression for Φ could not be solved analytically, so Φ was simulated. The space was first discretized by constructing a grid in the r and z directions with step sizes of Δr and Δz, respectively. Each point on the grid was assigned a set of values (i,j), where the i-index refers to points along "r" from the origin and the j-index refers to points along "z" from the origin. The physical boundaries of the permanent magnet were located at i* in the r direction and j* in the z direction. The boundaries of the entire grid, chosen to be 10 mm x 10 mm, were located at N_r in the r direction and N_z in the z direction. Space discretization intervals, Δr and Δz, were equal to each other and chosen to be 10 μm. The magnetization of the permanent magnet was 9.788 x 10^5 A m^{-1}. In order to simulate Φ, eqn (3) was approximated using finite difference values of first order derivatives and second order derivatives given by eqn (S1) and (S2), respectively.

$$\frac{\partial u}{\partial x} = \frac{u_{i+1} - u_{i-1}}{2\Delta x} \qquad \text{(S1)}$$

$$\frac{\partial^2 u}{\partial x^2} = \frac{u_{i+1} - 2u_i + u_{i-1}}{\Delta x^2} \qquad \text{(S2)}$$

After substitution of these approximations into eqn (3) and rearrangement, the general expression for $\Phi_{i,j}$ (i,j ≠0) was given by:

$$\Phi(i,j) = \frac{1}{4}\left[\left(1 + \frac{\Delta z^2}{2i\Delta r}\right)\Phi(i+\Delta r,j) + \left(1 + \frac{\Delta z^2}{2i\Delta r}\right)\Phi(i-\Delta r,j) + \Phi(i,j+\Delta z) + \Phi(i,j-\Delta z)\right] \qquad \text{(S3)}$$

Based on the geometry and the properties of the permanent magnet, the appropriate boundary conditions were given by:

$$\Phi(i,0) = 0 \qquad \text{(S4)}$$

$$\Phi(0,j) = \frac{1}{6}\left[4\Phi(\Delta r,j) + \Phi(0,j+\Delta z) + \Phi(0,j-\Delta z)\right] \qquad \text{(S5)}$$

$$\Phi(i^*,j) = \frac{1}{2}\left[\Phi(i^* + \Delta r,j) + \Phi(i^* - \Delta r,j)\right] \qquad \text{(S6)}$$

$$\Phi(i,j^*) = \frac{1}{2}\left[|M|\Delta z + \Phi(i,j^* + \Delta z) + \Phi(i,j^* - \Delta z)\right] \quad \text{(S7)}$$

$$\Phi(i^*,j^*) = \frac{1}{2}\left[\frac{1}{2}\left[|M|\Delta z + \Phi(i^*,j^* + \Delta z) + \Phi(i^*,j^* - \Delta z)\right] + \frac{1}{2}\left[\Phi(i^* + \Delta r,j^*) + \Phi(i^* - \Delta r,j^*)\right]\right] \quad \text{(S8)}$$

$$\Phi(N_r,N_z) = \frac{V|M|z}{4\pi r^3} \quad \text{(S9)}$$

The grid was first initialized by setting an arbitrary value for $\Phi_{i,j}$ everywhere ($\Phi_{i,j}$ = 1). The values of Φ were then calculated at the boundaries of the permanent magnet and the grid. The values of Φ at all other points on the grid are calculated iteratively based on the values of these boundaries. Due to the symmetry of the permanent magnet, calculations were performed only in the first quadrant and the values of Φ were applied to the remaining three quadrants with the corresponding positive or negative sign. Once the values for Φ are simulated, the first order derivative in eqn (S1) was used to determine the r- and z-components of H before obtaining the absolute value of H. The $\partial H/\partial z$ term in eqn (2) was then determined from the first order derivative of H in the z direction.

Supplemental Figures

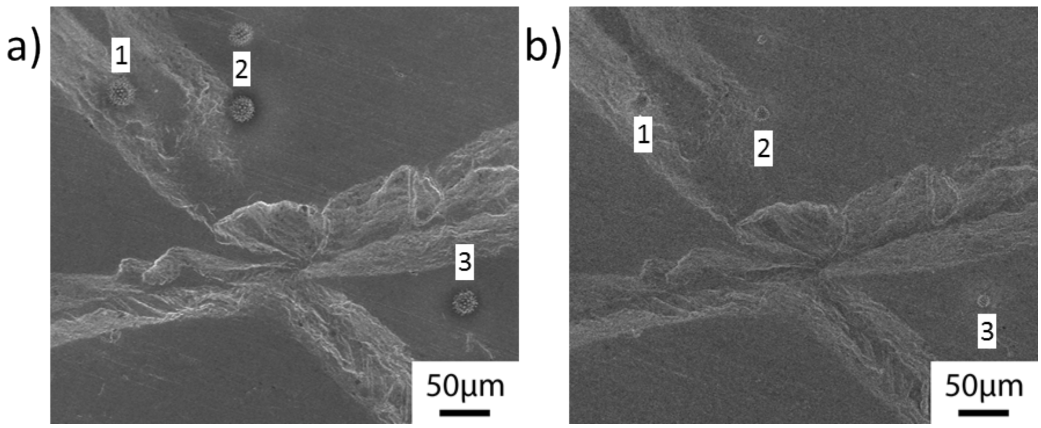

Fig. S1 SE images of Fe-O-coated pollen grains on nickel foil: a) before thermal treatment (after 30 SSG cycles and drying) and b) after thermal conversion (at 600°C, 4 h, air) into Fe_2O_3 sunflower pollen replicas.

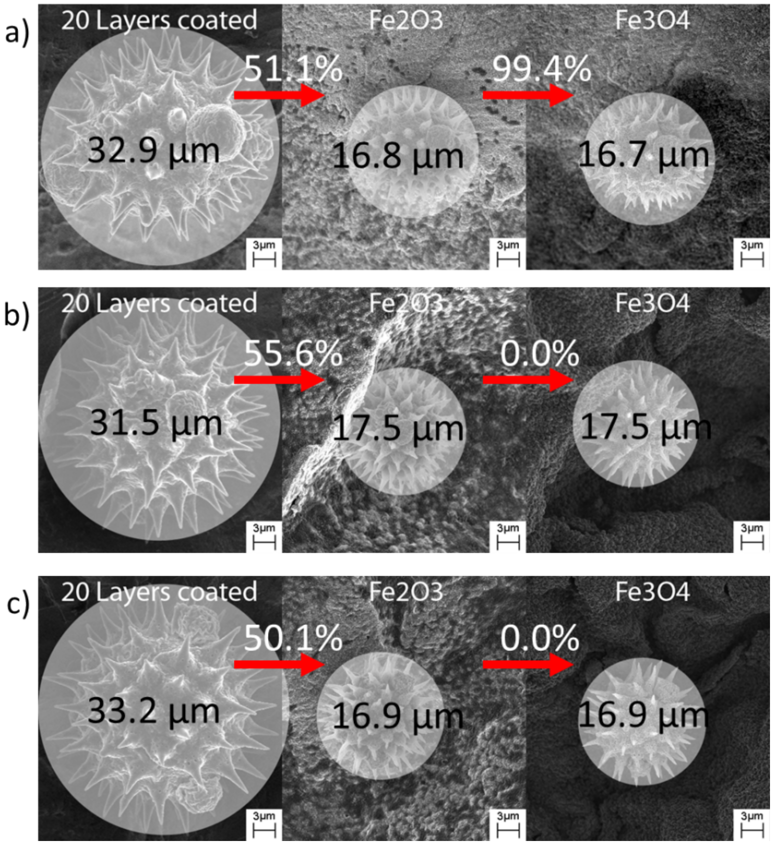

Fig. S2 SE images illustrating how the diameters of 3 particular coated pollen grains were determined at various stages of conversion into Fe_3O_4. Each of these as-coated particles was exposed to 20 SSG deposition cycles. A translucent circle was fitted around a given as-coated or thermally-treated pollen grain and the diameter of this circle was used as a measure of the pollen or pollen replica diameter.

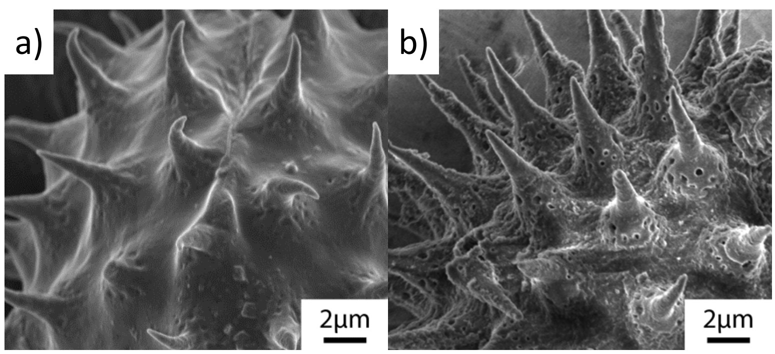

Fig. S3 SE images of the surfaces of: a) a cleaned sunflower pollen particle and b) a sunflower pollen particle exposed to 10 SSG deposition cycles.

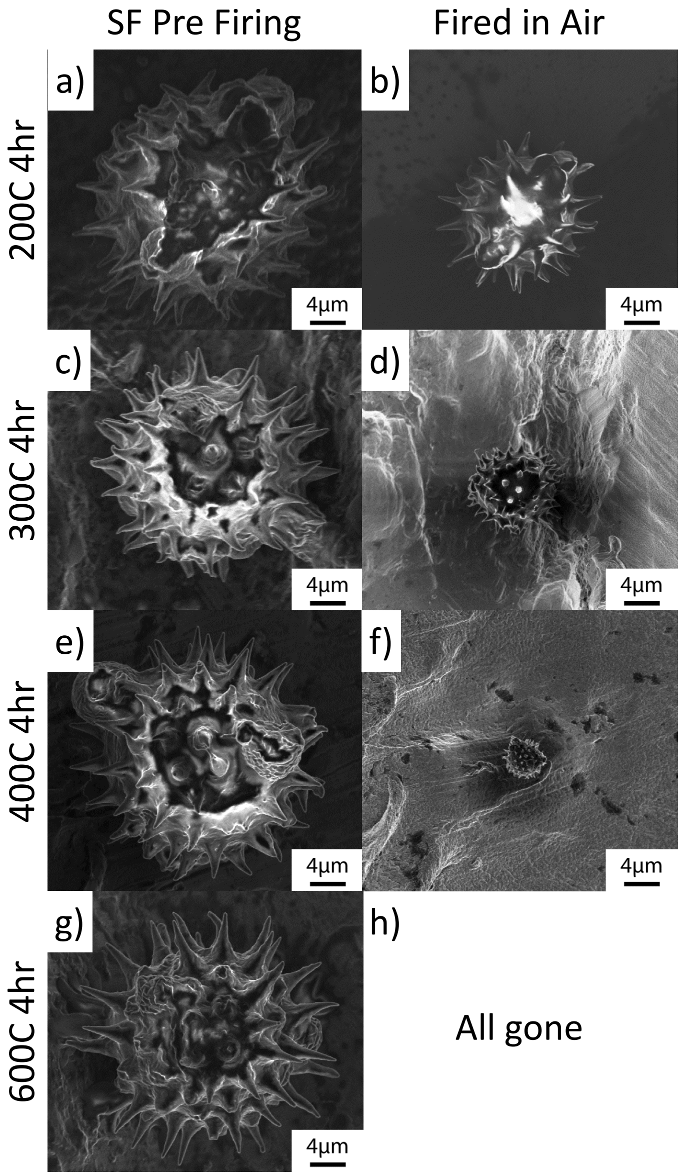

Fig. S4 SE images of: a), c), e), and g) cleaned sunflower pollen grains and the same grains after pyrolysis in air for 4 h at b) 200°C, d) 300°C, f) 400°C, or h) 600°C respectively.

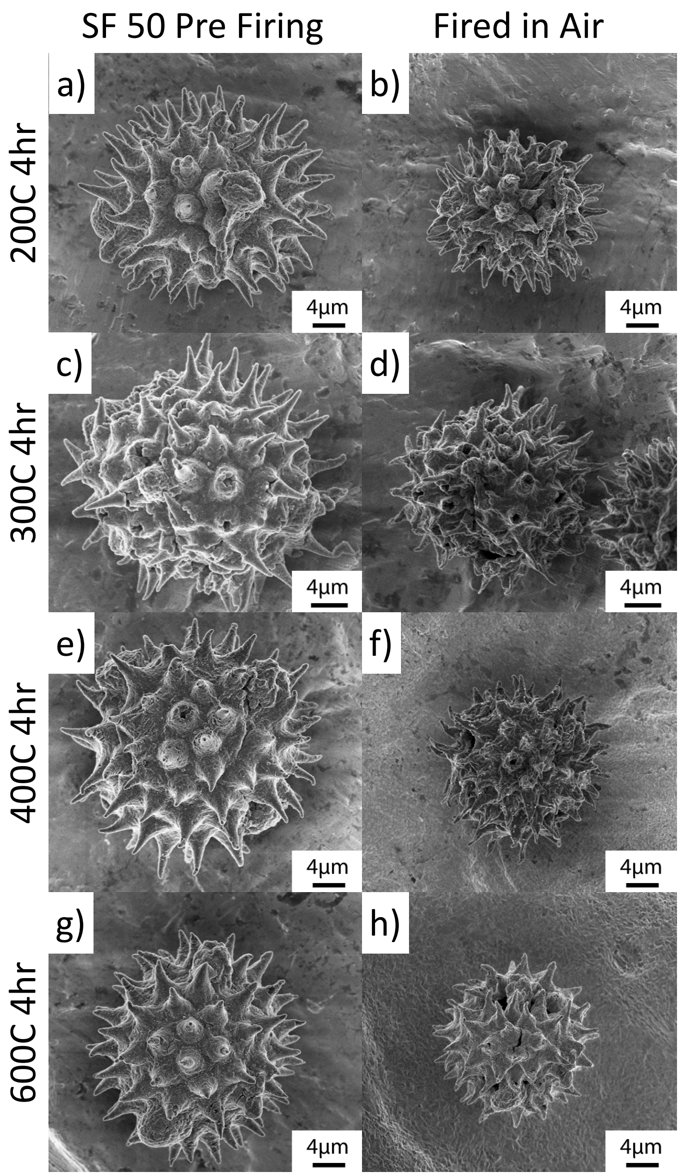

Fig. S5 SE images of: a), c), e), and g) sunflower pollen grains that had been coated via exposure to 50 SSG deposition cycles and the same grains after pyrolysis in air for 4 h at b) 200°C, d) 300°C, f) 400°C, or h) 600°C, respectively.

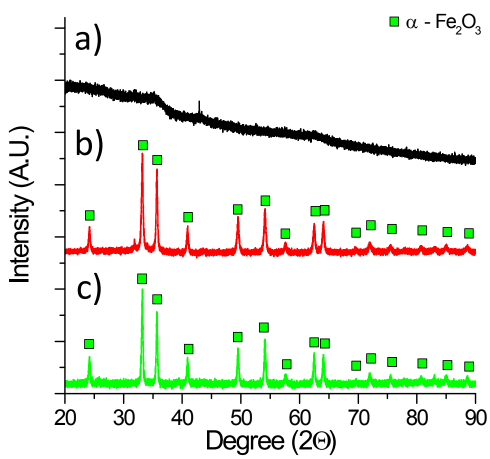

Fig. S6 XRD analyses of Fe-O-coated (50 SSG cycles) sunflower pollen grains after thermal treatment for 4 h in air at: a) 200°C, b) 300°C, or c) 600°C.

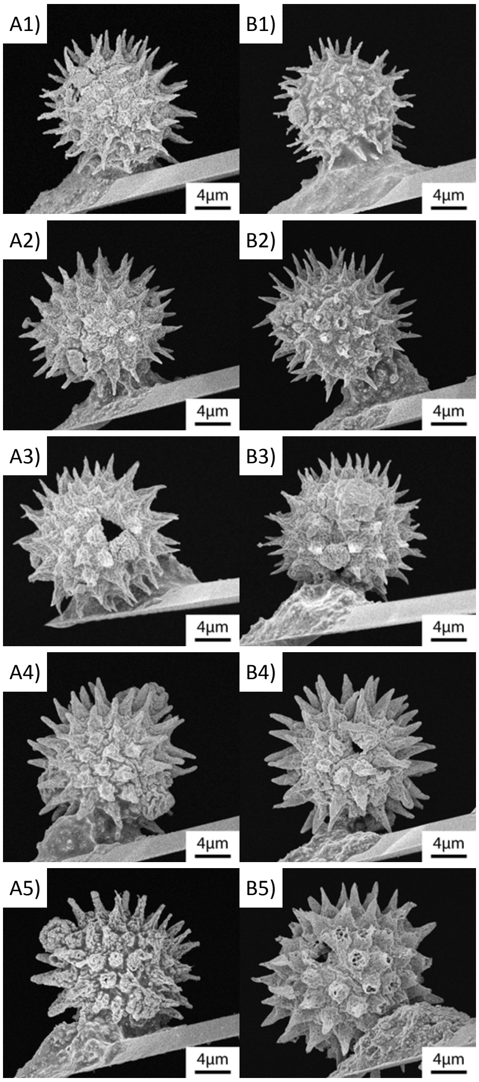

Fig. S7 SE images of single-particle-bearing cantilever probes of: A) Fe_2O_3 sunflower pollen replicas and B) Fe_3O_4 sunflower pollen replicas used in the AFM adhesion studies. Label "1" indicates 10 SSG cycles, label "2" indicates 20 SSG cycles, label "3" indicates 30 SSG cycles, label "4" indicates 40 SSG cycles, and label "5" indicates 50 SSG cycles.

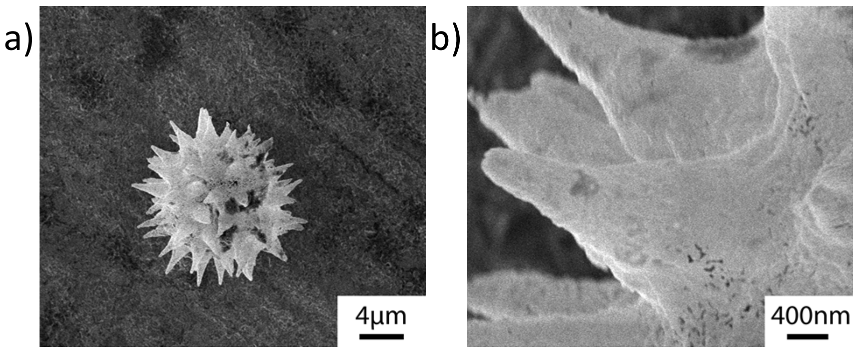

Fig. S8. SE images of a freestanding Fe_2O_3 sunflower pollen replica generated by exposure of the pollen to 2 SSG deposition cycles and then pyrolysis of the underlying pollen template for 4 h at 600^{o}C in air.

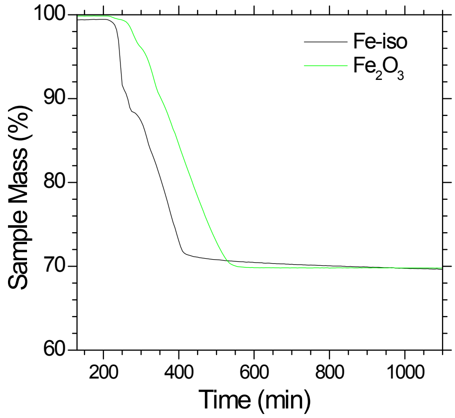

Fig. S9. Thermogravimetric analyses of hydrolyzed Fe(III) isopropoxide powder (“Fe-iso”) and bulk Fe_2O_3 powder (“Fe_2O_3”) upon heating at 5°C/min to 1100°C in a flowing 2%H_2/98%Ar atmosphere. The “Fe-iso” powder was generated by exposure of the Fe(III) isopropoxide precursor to DI water for 5 min at room temperature (i.e., under similar conditions as the hydrolysis step of the surface sol-gel deposition process). The observed weight losses for both powders were similar to the expected weight loss (30.1%) for the reduction of fully-oxidized iron oxide to elemental iron, which confirmed that the iron in the hydrolyzed iron alkoxide was fully oxidized.

Supplemental Tables:

Table S1 Average surface roughness (Ra, in nm) of the substrates

Si	PVA	PVAc	PS	Ni	Ni-Nd
0.2 ± 0.06	1.3 ± 0.03	0.3 ± 0.06	0.3 ± 0.02	2.7 ± 0.7	2.8 ± 0.4

Table S2 Values of the magnetite volume (V_m) obtained (eqn (2)) from a particular Fe_3O_4 pollen replica particle (generated with the use of 50 SSG deposition cycles) via magnetic force measurements as a function of distance from the magnetic Ni-Nd substrate. The final value of V_m was obtained by averaging magnetic volumes calculated over the initial 451 μm of retraction from the Ni-Nd substrate surface. At this distance (~25% of the maximum force of attraction), deviations that may occur when the measured magnetic force values approach the sensitivity of the AFM were avoided.

Distance (μm)	V_m (μm^3)
0	229
50	221
101	230
150	231
200	241
250	240
301	245
351	243
401	253
451	260